2001-01-1452

Vibration Power Transmission Through Multi-Dimensional Isolation Paths over High Frequencies

Seungbo Kim and Rajendra Singh
The Ohio State University

ABSTRACT

In many vibration isolation problems, translational motion has been regarded as a major contributor to the energy transmitted from a source to a receiver. However, the rotational components of isolation paths must be incorporated as the frequency range of interest increases. This article focuses on the flexural motion of an elastomeric isolator but the longitudinal motion is also considered. In this study, the isolator is modeled using the Timoshenko beam theory (flexural motion) and the wave equation (longitudinal motion), and linear, time-invariant system assumption is made throughout this study. Two different frequency response characteristics of an elastomeric isolator are predicted by the Timoshenko beam theory and are compared with its subsets. A rigid body is employed for the source and the receiver is modeled using two alternate formulations: an infinite beam and then a finite beam. Power transmission efficiency concept is employed to quantify the isolation achieved. Further, vibration power components are also examined. The roles of isolator parameters such as the static stiffness ratios, shape factors and material properties are investigated.

INTRODUCTION

Vibration isolators are often characterized as discrete elastic elements, with or without viscous or hysteritic damping [1-4]. The compressional stiffness term is typically used to develop isolation system models [2-4] though the transverse (shear) and rotational components are also sometimes specified or included [5-7]. Additionally, at higher frequencies, inertial or standing wave effects occur within the isolator [8-9]. Nonetheless, the isolators are still modeled by many researchers in terms of spectrally-invariant discrete stiffness elements without any cross-axis coupling terms [5-7]. Such descriptions are clearly inadequate at higher frequencies. Consequently, one must adopt the distributed parameter approach. It is the main focus of this article. Only a few articles have examined the elastomeric devices using the continuous vibration system theories [10-15]. For example, the longitudinal stiffness of an isolator has been described by the wave equation to characterize the material property of an isolator [10-13]. Also, rubber-like material has been modeled using the wave closure relationship [14]. The Euler beam theory has been adopted to describe the flexural motions of a mount for an active vibration control system [10, 11] and to characterize an isolator [12]. However, no prior article has examined the shear deformation and rotary inertia effects of an isolator. Further, the influence of component parameters on the behavior of an isolation system has been investigated using a standing wave description in the longitudinal direction and a static stiffness term in the flexural direction [14]. Yet, the frequency-dependent characteristics of an isolator have not been considered in previous isolation studies. This article proposes to overcome this particular void in the literature. Vibration transmitted via multi-dimensional motions of an isolator is conceptually shown in Figure 1 in the context of source, path (isolator) and receiver.

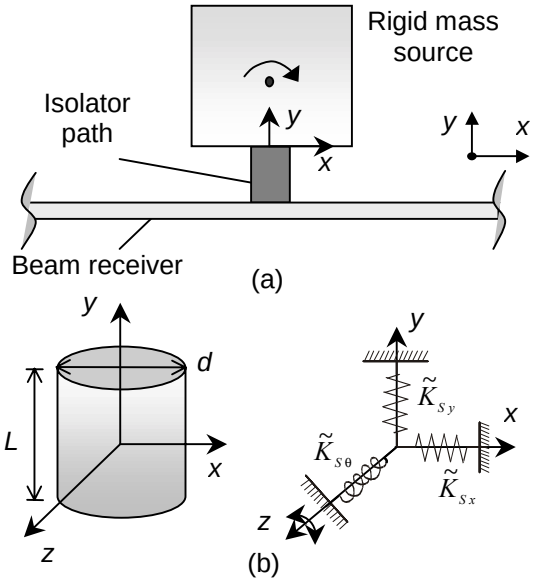

Figure 1. Vibration transmission via multi-dimensional motions of an isolator. (a) System configuration with a beam receiver; (b) a cylindrical isolator with static stiffness components used for parametric studies. Here, K_{Sy} is the axial (longitudinal or compressional) stiffness, K_{Sx} is the lateral (shear) stiffness and $K_{S\theta}$ is the rotational stiffness.

Primary objectives of this study are as follows. 1. Develop the frequency response characteristics (mobility or stiffness) of an isolator based on the continuous system theory that includes Timoshenko beam (in the transverse *x* direction) and the longitudinal (*y*) wave equation formulation. In particular, critically examine two types of solutions to the Timoshenko beam for a cylindrical rubber material. 2. Investigate the role of isolator parameters such as the static stiffness ratios, shape factors and material properties on isolation measures over a broad range of frequencies.

MOBILITIES OF TIMOSHENKO BEAM

The classical Timoshenko beam theory that describes the effects of shear deformation and rotary inertia has been well studied by many researchers [16-19]. Literature shows that there are two types of solution and two modal functions exist at high frequencies [17]. However, the high frequency solution has been ignored by many since this phenomenon has been believed to occur only at extremely high frequencies [16]. Only a few studies have been conducted to examine the dispersion and spectrum relations of the Timoshenko beam structure at high frequencies [18, 19]. In our study, we examine this issue and the characteristic mobilities are obtained for a semi-infinite elastomeric beam. Detailed mathematical treatment is given in the recent journal article we wrote [20]. It is assumed that the shear modulus (*G*) is very low that is true for a rubber-like material. The example case considers a rubber beam with circular shape. The spectrally-invariant material properties and dimensions of the beam that is considered as an isolator are shown in Table 1.

Table 1. Material properties and dimensions of source, isolator and receiver system.

Property or dimension	Source (Cubic rigid body)	Isolator: baseline (Circular beam)	Receiver (Rectangular beam)
m (kg)	1	-	-
E (MPa)	-	1.62	6.688 X 10^4
G (MPa)	-	5	-
η	-	0.3	0.001
ρ (kg/m^3)	-	1000	2723
Dimensions in mm	*L* = 50	*L* = 30 *r* = 12	*L* = 670 (finite beam) *b* = 100 and *t* = 10 (finite or infinite beam)

The effects of shear deformation and rotary inertia on the characteristic mobilities for a semi-infinite rubber beam are examined and shown in Figure 2.

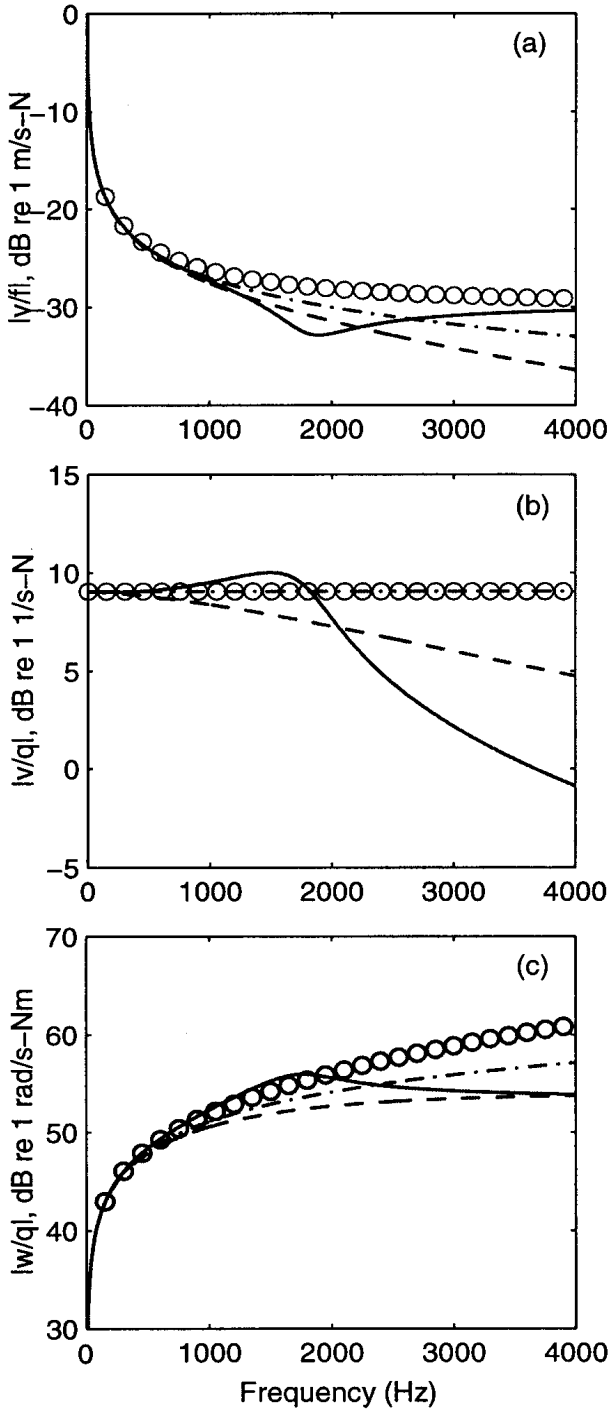

Figure 2. Characteristic mobilities of a semi-infinite beam. (a) Force mobility $|v/f|$; (b) coupling mobility $|v/q|$; (c) moment mobility $|w/q|$. Key: ——— , Timoshenko beam; o , Euler beam with shear deformation;------, Euler beam with rotary inertia;–·–·–, classical Euler beam. Here, ω_T is 1700 Hz.

Note that the frequency response characteristics of a Timoshenko beam changes at the transition frequency (ω_T). Details are given in reference [20]. It is observed from Figure 2 that the inclusion of shear deformation increases the magnitudes of force and moment mobilities. Conversely, the rotary inertia decreases the magnitudes of force and moment mobilities. Further, the shear deformation does not affect the coupling mobility of Figure 2(b) that is frequency-invariant for the Euler beam model and the one with shear deformation only. For this circular rubber beam, ω_T is approximately 1.7 kHz and the nature of spectra changes beyond this transition. Beyond ω_T, the characteristic force and moment mobilities of Timoshenko beam model remain frequency-invariant as the frequency increases, unlike the Euler beam model. Further, the coupling mobility decreases by the rotary inertia effect and the one of the Timoshenko beam solution decreases more rapidly beyond ω_T. Also, the coupling mobilities of the Euler beam with or without shear deformation are the same as shown in Figure 2(b).

TRANSMITTED VIBRATION POWER FROM SOURCE TO RECEIVER AND EFFICIENCY

The time-averaged vibrational power (Π) components transmitted to a beam receiver are obtained by using harmonic responses and interfacial forces (*F* and *V*) and moment (*M*). Define Π_x, Π_y and Π_θ as the lateral (*x*), axial (*y*) and rotational (θ) power components respectively:

$$\Pi_x(\omega) = \frac{1}{2} Re[\,\tilde{F}(\omega)\,\tilde{v}_x^*(\omega)\,] = \frac{1}{2} Re[\,\tilde{v}_x(\omega)\,\tilde{F}^*(\omega)\,], \quad (1a)$$

$$\Pi_y(\omega) = \frac{1}{2} Re[\,\tilde{V}(\omega)\,\tilde{v}_y^*(\omega)\,] = \frac{1}{2} Re[\,\tilde{v}_y(\omega)\,\tilde{V}^*(\omega)\,], \quad (1b)$$

$$\Pi_\theta(\omega) = \frac{1}{2} Re[\,\tilde{M}(\omega)\,\tilde{w}^*(\omega)\,] = \frac{1}{2} Re[\,\tilde{w}(\omega)\,\tilde{M}^*(\omega)\,]. \quad (1c)$$

Here, v_x, v_y and w are the axial (shear direction *x* for isolator), vertical (axial direction *y* for isolator) and rotational (θ) velocity amplitudes of the receiver beam respectively. Finally, the total vibration power transmitted to a receiver beam is

$$\Pi_{\text{Total}}(\omega) = \Pi_x(\omega) + \Pi_y(\omega) + \Pi_\theta(\omega). \quad (2)$$

Additionally, define vibration power transmission efficiency as

$$\Gamma(\omega) = \frac{\Pi_{\text{Total}}(\omega)}{\Pi_{\text{IN}}(\omega)}. \quad (3)$$

where Π_{IN} is the harmonic power supplied to a rigid body source.

VIBRATION POWER TRANSMITTED TO AN INFINITE BEAM RECEIVER

SYSTEM CONFIGURATION: The vibrational behavior is examined for an isolation system (Figure 1a) with an infinite beam receiver. Harmonic excitation is applied at the mass center of a cubic rigid body. Circular isolator is shown in Figure 1(b) along with vibration components transmitted through the path. The isolator is modeled using the Timoshenko beam theory (flexural motion) and the wave equation (longitudinal motion). Note that the coupling mobility does not exist for an infinite beam receiver. However, a coupling arises because the motion (or force) in shear direction of an isolator is coupled with the longitudinal direction of a receiver beam. Material properties of the isolator are listed in Table 1. The Young's modulus E_P for a rubber material is found from the relation $E_P = 3G_P(1+QT^2)$ where *Q* is an empirical constant and *T* is the shape factor. For a circular rubber cylinder, *Q* is 2 and *T* is equal to $2r/(4L_P)$ where *r* and L_P are the radius and length of the isolator beam respectively [16]. Also, a frequency-invariant loss factor η_P is included in the calculation with the complex-valued Young's modulus as $\tilde{E}_P = E_P(1+j\eta_P)$ to incorporate hysteretic damping within the isolator. Material properties of the receiver beam are, as well the dimensions of source, also shown in Table 1. A loss factor η_R of 0.001 is used to represent a lightly damped structure and included in the complex-valued $\tilde{E}_R$. Given the system properties, the effects of isolator material and geometric properties on the vibration power transmitted to receiver are examined.

EFFECT OF ISOLATOR PROPERTIES ON VIBRATION POWER TRANSMISSION: In order to understand the effect of isolator properties, it is useful to examine static stiffnesses (K_S) of isolator. It should be noted that flexural stiffnesses have to be dealt with in a matrix form since there exist coupling terms between lateral (shear *x*) and rotational (θ) stiffnesses. Further, note that *G* (or *E*) is common to all stiffness terms. Highly damped material with a loss factor of 0.3 is used for this isolator so that overall frequency-dependent characteristics are observed without the influence of isolator resonances. Results for Γ are shown in Figure 3(a) for a variation in *G* values for an isolator when a harmonic moment is applied to the mass center of a rigid body source. It is observed in Figure 3(a) that Γ rises due to an increase in *G* as the frequency increases. Additionally, the Γ spectra of Figure 6(a) decrease as the frequency increases. The power efficiency is also shown in Figure 3(b) when a harmonic force (f_y) is applied to the mass center of a source. In this case, only axial stiffness of the mount affects vibration power transmission. Like the moment application case, Γ grows with *G* as the frequency increases. Also, note that the Γ spectra of Figure 3(b) for the axial power transmission are close to unity at low frequencies unlike the one of Figure 3(a) for the flexural power transmission. Normalized power components with respect to the total actual power transmitted to the receiver beam are also shown in Figures 4 for the shear modulus variation.

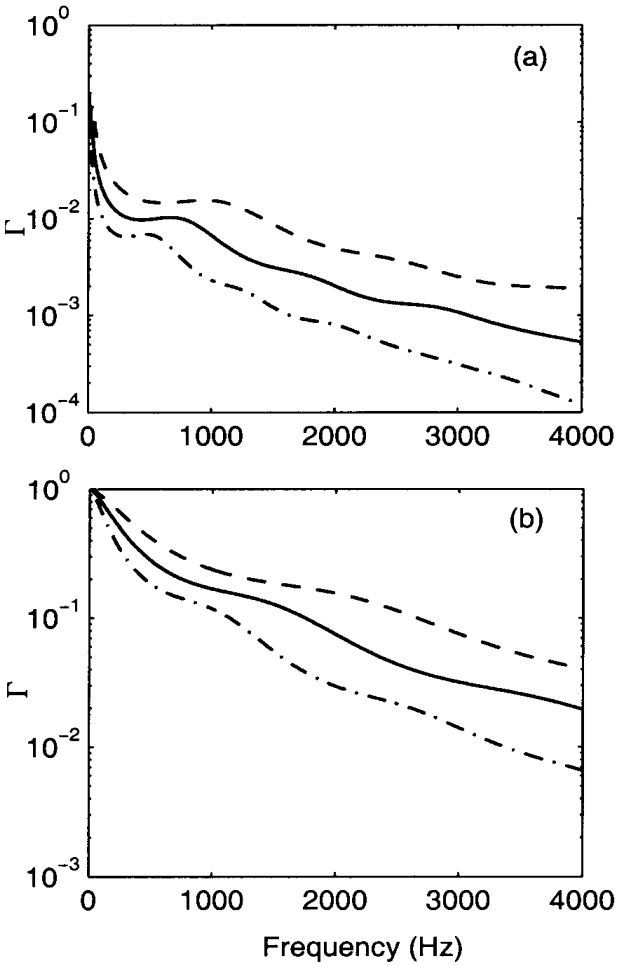

Figure 3. Effect of shear modulus *G* of an isolator on efficiency (Γ) with an infinite beam receiver. (a) For a Timoshenko beam isolator model given moment excitation; (b) given force excitation f_y. Key: –·–·–, 0.5*G*; ———, *G*; - - - - - -, 2*G*.

As discussed previously, axial and coupling power components do not exist in this case and therefore the sum of the normalized lateral (shear direction of mount) and rotational power components is equal to unity. Overall, the lateral power component is larger than the rotational component. It is shown in Figure 4(b) that the lateral component dominates.

Commonly, designers specify mounts in terms of lumped stiffness elements rather than continuous system properties. Therefore, the following static stiffness ratios (α) are defined. Here, each ratio is normalized with respect to the axial component:

$$\alpha_{xy} = \frac{K_{Sx}}{K_{Sy}}, \qquad \alpha_{cy} = \frac{K_{Sx}}{K_{Sy}}, \qquad \alpha_{\theta y} = \frac{K_{Sx}}{K_{Sy}}. \quad \text{(4a-c)}$$

where α_{xy}, α_{cy} and $\alpha_{\theta y}$ are the ratios of shear, coupling and rotational stiffness components to the axial stiffness respectively. For a cylindrical isolator, key parameters in the static flexural stiffnesses include the slenderness ratio (S/L), material properties (*G* and v) and K_{Sy}. In this case, the flexural stiffnesses change when *L* is varied proportionally to *S*, unlike the K_{Sy} value.

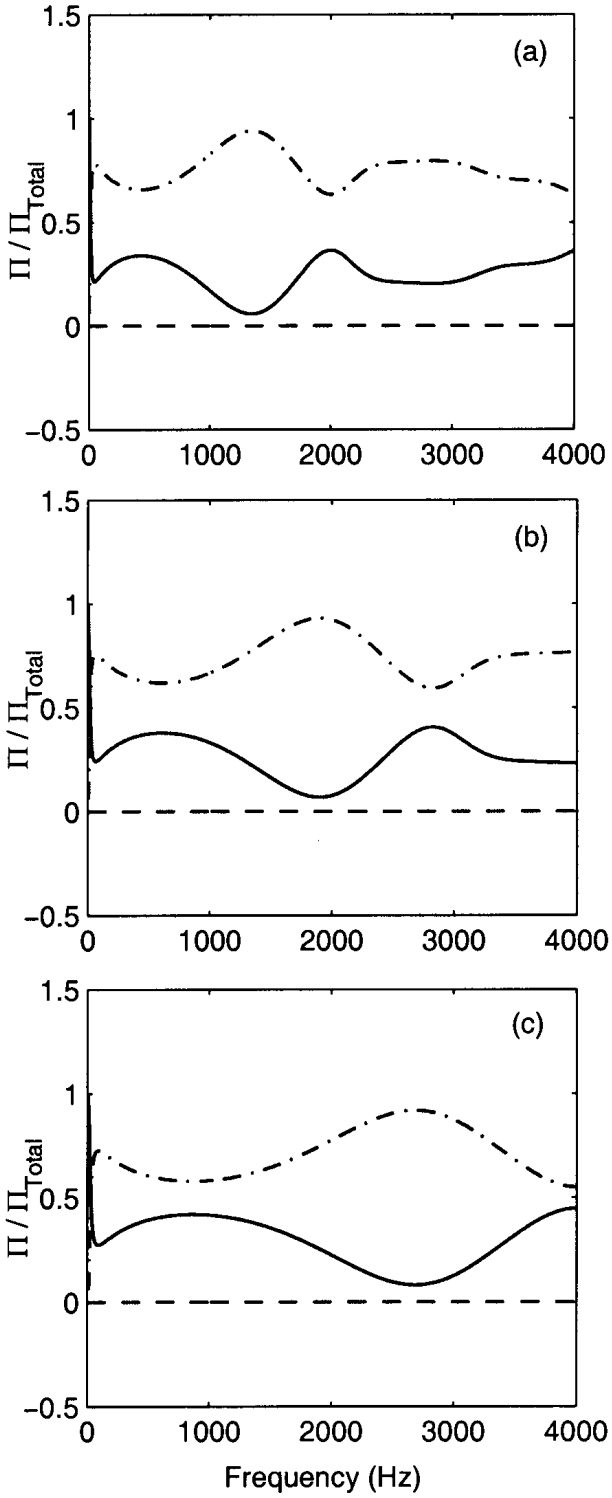

Figure 4. Normalized vibration power transmitted to an infinite beam given moment excitation. (a) 0.5G; (b) G; (c) 2G. Key: - - - - - -, axial (y); ———, rotational (θ); –·–·–, lateral (x).

Note that this behavior is also true for the Euler beam case. Further, α_{xy} decreases but both α_{cy} and $\alpha_{\theta y}$ increase as *L* or *S* value is increased, while holding S/L, G and v. The effects of α_{xy} on efficiency (Γ) are examined in Figure 5 for the case when *L* is proportionally varying with *S*.

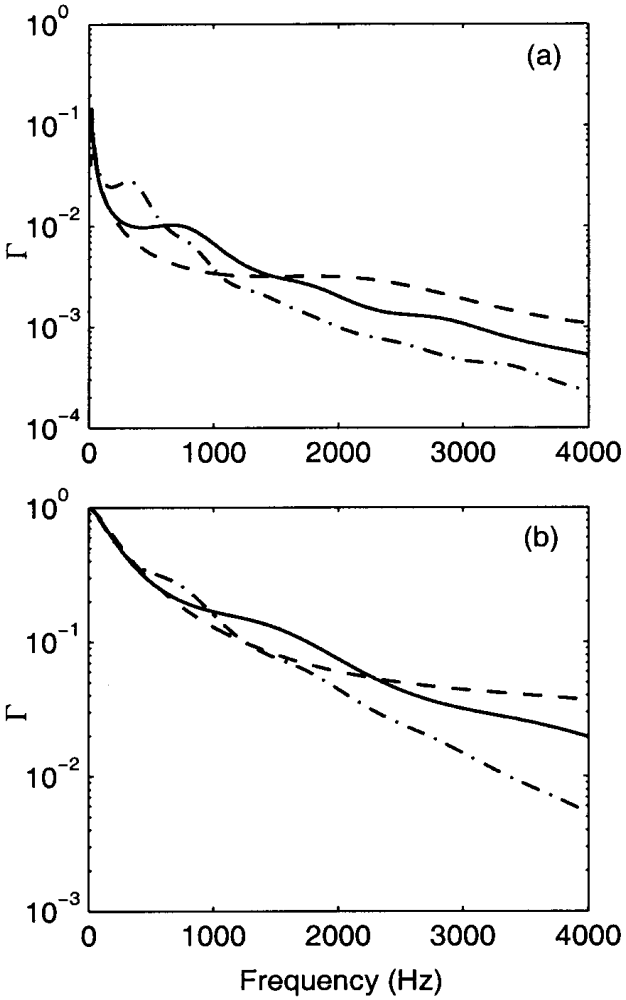

Figure 5. Effect of α_{xy} (ratio of shear to axial components of static stiffness) of an isolator on efficiency (Γ) with an infinite beam receiver. (a) For a Timoshenko beam isolator model given moment excitation; (b) given force excitation f_y. Key: –·–·– , $0.7\,\alpha_{xy}$; ———, α_{xy}; ------, $1.3\,\alpha_{xy}$.

Figure 5(a) shows that Γ increases as α_{xy} is increased at higher frequencies when a harmonic moment is applied at mass center of a source. Note that the minimum value of α_{xy} produces the best vibration isolation (hence the lowest Γ) for a system with a Timoshenko beam isolator as shown in Figure 5(a). The Γ spectra are shown in Figure 5(b) when a harmonic force (f_y) is applied to a source. Note that K_{Sy} is the only component that affects the power transmission and K_{Sy} is unchanged as α_{xy} is varied in this case. As expected, Γ remains unchanged for the α_{xy} variations at lower frequencies. However, it is observed in Figure 5(b) that Γ increases as α_{xy} increases at higher frequencies. Similar to the previous case, vibration power components are calculated in Figure 6. The dominance of lateral and rotational power components changes at certain frequency for the lowest α_{xy} value as shown in Figures 6(a).

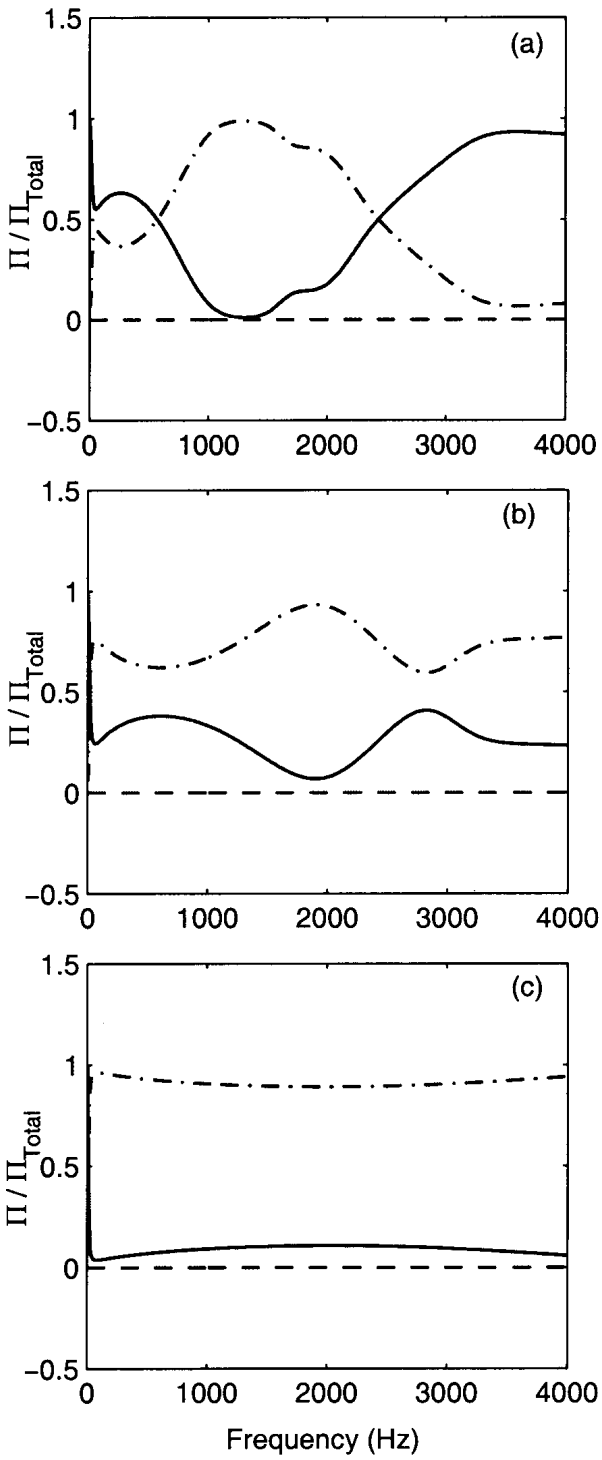

Figure 6. Normalized vibration power transmitted to an infinite beam given moment excitation. (a) $0.7\,\alpha_{xy}$; (b) α_{xy}; (c) $1.3\,\alpha_{xy}$. Key:------, axial (y); ——— , rotational (θ);–·–·–, lateral (x).

Observe for the lowest α_{xy} value case that the rotational power component is dominant at lower frequencies and continues to dominate up to the mid-frequency regime where the lateral component is important. However, the lateral component becomes more significant when α_{xy} is increased and the rotational component is negligible for the highest α_{xy} case. Next, the effects of the isolator

shape on isolation measures are examined. The shape factor (β) of an isolator is defined as $\beta = L/d$. Note that an increase in β reduces the static flexural and axial stiffnesses. Results are shown in Figure 7.

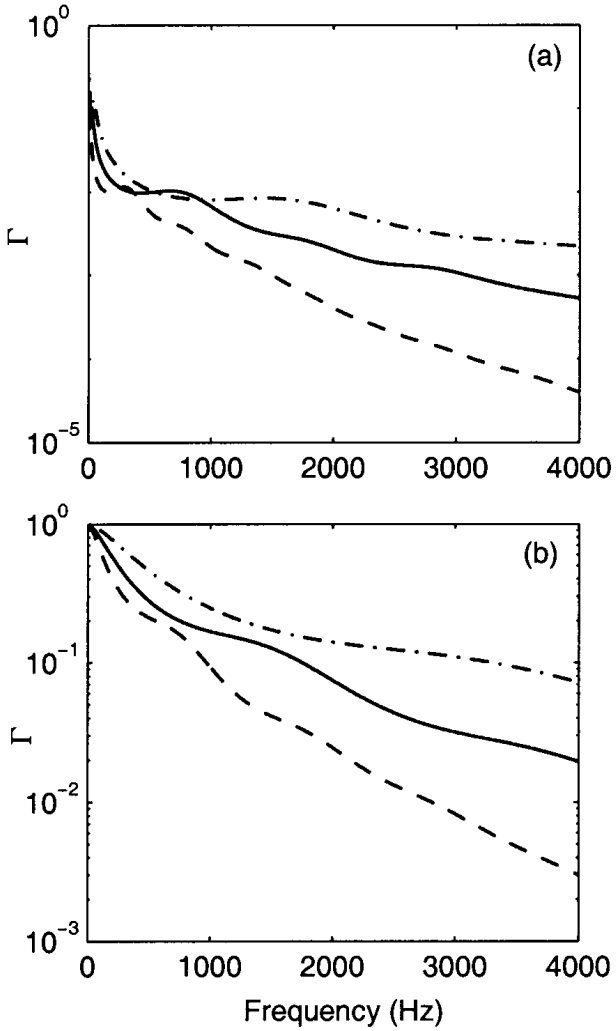

Figure 7. Effect of isolator shape factor β on efficiency (Γ) with an infinite beam receiver. (a) For a Timoshenko beam isolator model given moment excitation; (b) given force excitation f_y. Key:—·—·—, 0.5β; ———, β; - - - - - -, 2β.

The Γ value decreases at higher frequencies as β is increased when a moment is applied. Similar to the moment excitation case, Γ decreases at higher frequencies as β is increased for a force (f_y) excitation case as shown in Figure 7(b). Normalized vibration power components are also shown in Figure 8. Like the previous cases, the lateral component is larger than the rotational component over all frequencies. However, the rotational component becomes more important at lower and higher frequencies as β is increased.

VIBRATION POWER TRANSMITTED TO A FINITE BEAM RECEIVER

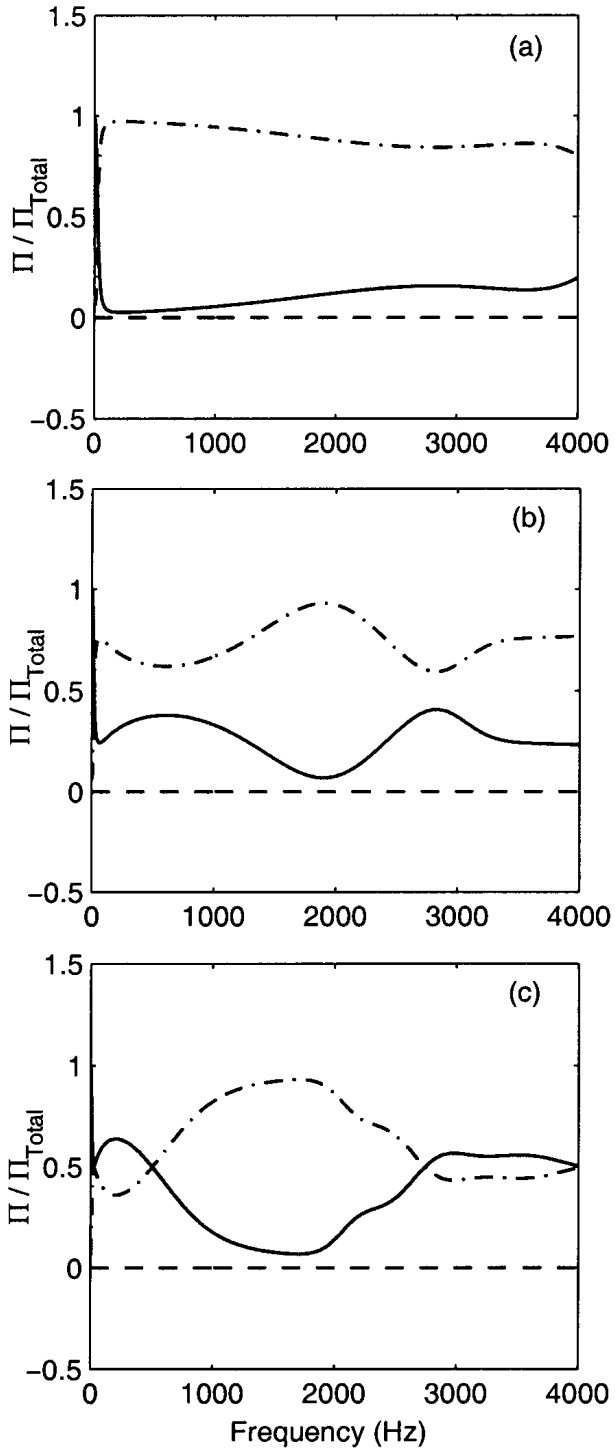

Figure 8. Normalized vibration power transmitted to an infinite beam given moment excitation. (a) 0.5β; (b) β; (c) 2β. Key: - - - - - -, axial (y); ———, rotational (θ); —·—·—, lateral (x).

A finite beam receiver (with clamped ends) is employed to examine the vibration transmission through the isolator for a system of Figure 1(a). Similar to the system with an infinite beam receiver, the Timoshenko beam model represent flexural motion of an isolator along with the wave equation for longitudinal motion. An isolator connected to a rigid body source at one end is assumed to be located off-center ($L_{RI} = 3L_R/4$) of the receiver

beam in order to incorporate the effect of coupling mobility of the receiver beam. Note that such a coupling mobility does not exist for a centrally driven beam (with both ends clamped) and for an infinite beam. The effects of *G* of a Timoshenko beam isolator on Γ are shown Figure 9(a) when a moment is applied at a source.

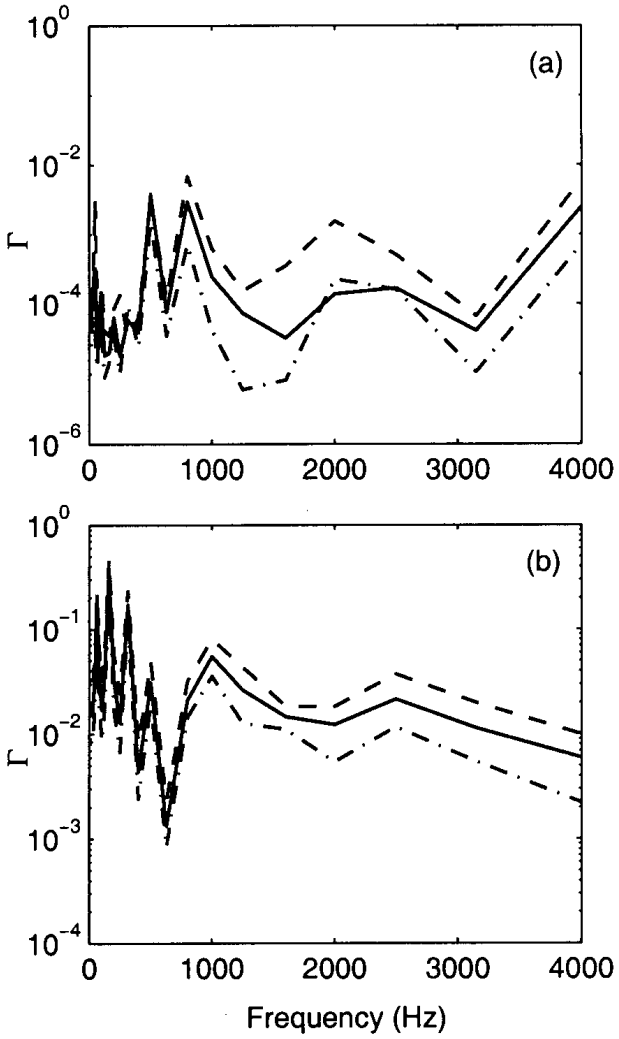

Figure 9. Effect of isolator *G* on efficiency (Γ) with a finite beam receiver. (a) For a Timoshenko beam isolator model given moment excitation; (b) given force excitation f_y. Key:—·—·—, 0.5*G*; ———, *G*; ———, 2*G*.

Like the infinite beam receiver case, Γ rises especially at higher frequencies as *G* of an isolator is increased. However, the deviation from the aforementioned behavior is observed at certain frequencies (around 2 kHz) due to the coupling mobility and resonances of the receiver beam. Like the system with an infinite beam receiver, Γ of the Timoshenko beam isolator shows the relatively flat spectra over the frequencies as shown in Figure 9(a). When a force f_y is applied to a source, Γ increases as *G* is increased as shown in Figure 9(b). Unlike the case of an infinite beam receiver, Γ is not close to unity at low frequencies.

Next, the effect of α_{xy} is examined while holding the slenderness and material properties of the mount. Results are shown in Figure 10 for a moment excitation case.

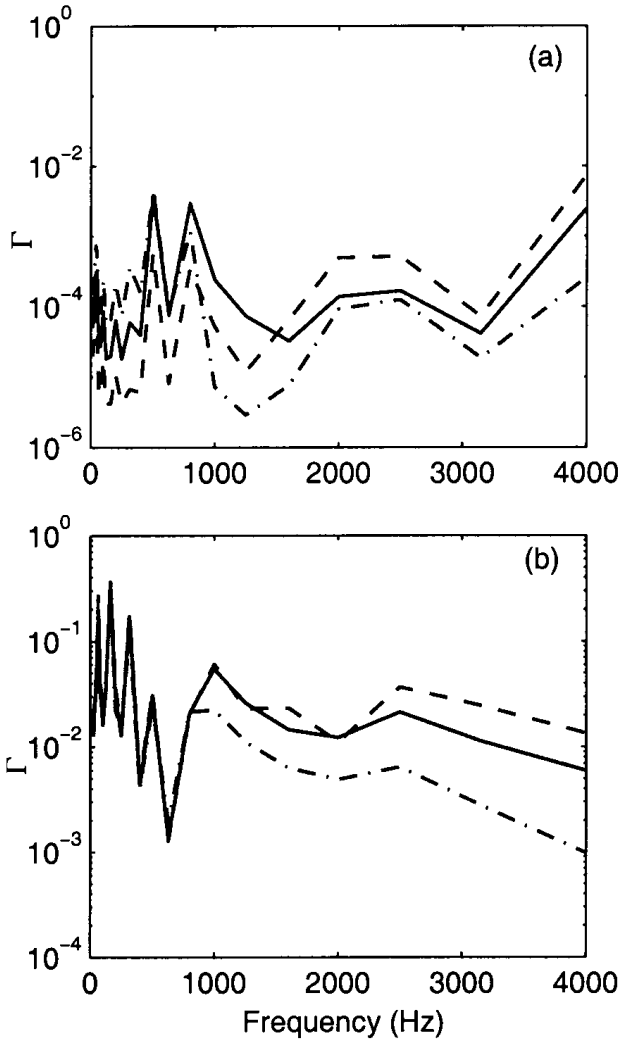

Figure 10. Effect of isolator α_{xy} on efficiency (Γ) with a finite beam receiver. (a) For a Timoshenko beam isolator model given moment excitation; (b) given force excitation f_y. Key:—·—·—, $0.3\,\alpha_{xy}$; ———, α_{xy}; - - - - - - , $1.3\,\alpha_{xy}$.

Similar to the infinite beam receiver case, Γ increases at higher frequencies as α_{xy} of the Timoshenko beam isolator is increased as shown in Figure 10(a). And, Γ is shown in Figure 10(b) when a force f_y is applied and observe that Γ increases at higher frequencies as α_{xy} is increased like the moment excitation case even though the static axial stiffness (K_{Sx}) plays a major role in this force excitation case; K_{Sx} is kept unchanged for all α_{xy} variations. Note that Γ remains unchanged up to a certain frequency (around 800 Hz in this case) as α_{xy} is varied, as shown in Figure 10(b). Finally, the effects of β on Γ are examined in Figure 11. Similar to the infinite

beam receiver case, an increase in β decreases Γ for both moment and force excitation cases.

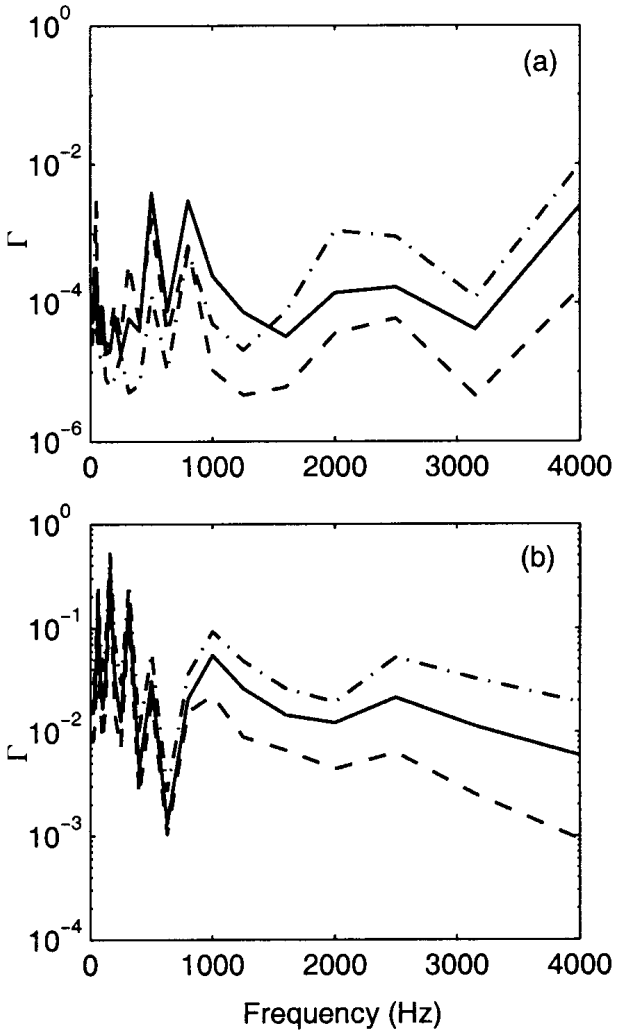

Figure 11. Effect of isolator shape factor β on efficiency (Γ) with a finite beam receiver. (a) For a Timoshenko beam isolator model given moment excitation; (b) given force excitation f_y. Key: —·—·—, 0.5β; ———, β; ------, 2β.

CONCLUSION

Chief contribution of this paper is the application of continuous system theory to an elastomeric isolator and the examination of associated flexural and longitudinal motions of the source-path-receiver system.Two different frequency response characteristics of an elastomeric isolator are predicted by the Timoshenko beam theory. The second type solution, that has been previously believed to occur at extremely high frequencies (say around 80 kHz) for metallic structures and therefore not of interest in structural dynamics, takes place at relatively low frequencies (say around 1.5 kHz) for a rubberlike material. The continuous system analysis clearly shows that the shear deformation and rotary inertia must be considered in order to properly describe the spectral behavior of mount in flexural motions at higher frequencies. In particular, the shear deformation effect is found to be more pronounced than the role of the rotary inertia at higher frequencies. The behavior of a typical vibration isolation system has been examined using the power transmitted to an infinite beam or a finite beam receiver, when excited by a harmonic moment or force at the source. Parametric study of isolator parameters on the transmission measures has been conducted using the Timoshenko beam isolator model and an infinite beam receiver. Material and geometric parameters of an isolator have been examined along with the static stiffness ratios (between K_{Sy}, K_{Sx} and $K_{S\theta}$ components). The vibration power efficiency for an isolation system with an infinite beam structure increase with frequency as the isolator shear modulus is increased. Resulting characteristics for a system with a finite beam receiver confirm the trends. Future work is required to quantify the vibration source in terms of power transmission. Proper interpretation of various vibration isolation measures for a multi-dimensional system, such as power efficiency and effectiveness, must also be sought over a broad range of frequencies. Finally, nonlinear effects of an isolator should be examined.

ACKNOWLEDGMENTS

The General Motors Corporation (Noise and Vibration Center) and the Goodyear Tire and Rubber Company (Transportation Molded Products) are gratefully acknowledged for supporting this research.

REFERENCES

1. T. JEONG and R. SINGH 2000 *Journal of Sound and Vibration*, Inclusion of Measured Frequency- and Amplitude-Dependent Mount Properties in Vehicle or Machinery Models (in press).
2. H. G. D. GOYDER and R. G. WHITE 1980c *Journal of Sound and Vibration*, **68**(1), 97-117. Vibrational Power Flow from Machines into Built-Up Structures, Part III: Power Flow Through Isolation Systems.
3. J. I. SOLIMAN and M. G. HALLAM 1968 *Journal of Sound and Vibration*, **8**(2), 329-351. Vibration Isolation between Non-Rigid Machines and Non-Rigid Foundations.
4. J. C. SNOWDON 1968 *Vibration and Shock in Damped Mechanical Systems*. New York: John Wiley & Sons, Inc.
5. M. A. SANDERSON 1996 *Journal of Sound and Vibration*, **198**(2), 171-191. Vibration Isolation: Moments and Rotations Included.
6. W. L. LI and P. LAVRICH 1999 *Journal of Sound and Vibration*, **224**(4), 757-774. Prediction of Power Flows Through Machine Vibration Isolators.
7. J. PAN, J. PAN and C. H. HANSEN 1992 *Journal of the Acoustical Society of America*, **92**(2), 895-907. Total Power Flow from a Vibrating Rigid Body to a Thin Panel Through Multiple Elastic Mounts.
8. E. UNGAR and C. W. DIETRICH 1966 *Journal of Sound and Vibration*, **4**(2), 224-241. High-Frequency Vibration Isolation.

9. M. A. BERANEK 1988 *Noise and Vibration Control*. Washington, DC: Institute of Noise Control Engineering.
10. P. GARDONIO, S. J. ELLIOTT and R. J. PINNINGTON 1997 *Journal of Sound and Vibration*, **207**(1), 61-93. Active Isolation of Structural Vibration on a Multiple-Degree-of-Freedom System, Part I: The Dynamics of the System.
11. P. GARDONIO, and S. J. ELLIOTT 2000 *Journal of Sound and Vibration*, **237**(3), 483-511. Passive and Active Isolation of Structural Vibration Transmission between Two Plates Connected by a Set of Mounts.
12. S. KIM and R. SINGH 2000 *Journal of Sound and Vibration*, Multi-Dimensional Characterization of Vibration Isolators over a Wide Range of Frequencies (in press).
13. L. F. NIELSEN, N. J. WISMER and S. GADE 2000 *Sound and Vibration,* February, 20-24. An Improved Method for Estimating the Dynamic Properties of Materials.
14. L. CREMER and M. HECKLE 1973 *Structure-Borne Sound: Structural Vibrations and Sound Radiation at Audio Frequencies*. New York: Springer-Verlag.
15. R. G. DEJONG, G. E. ERMER, C. S. PAYDENKAR and T. M. REMTEMA 1998 *Noise-Con 98* High Frequency Dynamic Properties of Rubber Isolation Elements.
16. J. C. SNOWDON 1968 *Vibration and Shock in Damped Mechanical Systems*. New York: John Wiley & Sons, Inc.
17. R. W. TRAILL-NASH and A. R. COLLAR 1953 *Quarterly Journal of Mechanics and Applied Mathematics*, **6**, 186-222. The effect of shear flexibility and rotary inertia on the bending vibrations of beams.
18. J. F. DOYLE 1997 *Wave Propagation in Structures: Spectral Analysis Using Fast Discrete Fourier Transforms*. New York: Springer-Verlag.
19. S. GOPALAKRISHNAN, M. MARTIN and J. F. DOYLE 1992 *Journal of Sound and Vibration*, **158**(1), 11-24. A Matrix Methodology for Spectral Analysis of Wave Propagation in Multiple Connected Timoshenko Beams.
20. S. KIM and R. SINGH 2001 *submitted to the Journal of Sound and Vibration*, Vibration Transmission Through an Isolator Modeled by Continuous System Theory.

LIST OF SYMBOLS

b	width
d	diameter
E	Young's modulus
f	force amplitude
F	axial force
G	shear modulus
j	$\sqrt{-1}$
K	stiffness
L	length
m	mass
M	moment
q	moment amplitude
Q	empirical constant for rubber
r	radius
S	area
t	thickness
T	shape factor for rubber material
v	translational velocity
V	shear force
w	rotational velocity
x, y, z	cartesian coordinates
α	static stiffness ratio
β	shape factor of isolator (L/d)
Γ	efficiency of vibration power
η	loss factor
θ	rotational displacement
ν	Poissons ratio
Π	vibration power (time-averaged)
ρ	mass density
ω	frequency, rad/sec
ω_T	transition frequency, rad/sec

Subscripts

c	coupling
IN	input
P	isolator (path)
R	receiver
RI	interfacial location of receiver beam with isolator
S	static
T	transition frequency
Total	sum of power components transmitted to receiver
x, *y*, *z*	cartesian coordinates
θ	rotational component

Superscripts

~	complex valued
*	complex conjugate

Operators

Re	real part

CONTACT

http://rclsgi.eng.ohio-state.edu/~singh/ADL.html